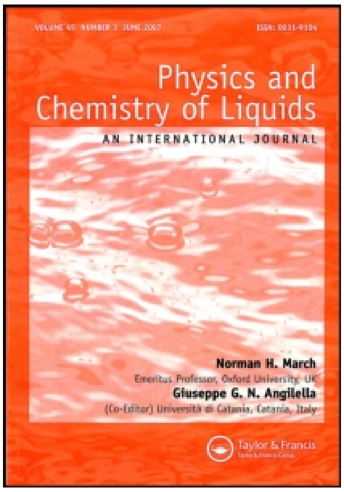

Physics and Chemistry of Liquids

Publication details, including instructions for authors and subscription information:
http://www.informaworld.com/smpp/title~content=t713646857

Charge Ordering and Size Effects in the Structure of a Model 2:1 Ionic Compound

J. Boronat[a]; M. Silbert[b]
[a] Departament de Física i Enginyeria Nuclear, Universitat Politècnica de Catalunya, Barcelona, Spain [b] School of Physics, University of East Anglia, Norwich, U.K.

To cite this Article Boronat, J. and Silbert, M.(1994) 'Charge Ordering and Size Effects in the Structure of a Model 2:1 Ionic Compound', Physics and Chemistry of Liquids, 27: 2, 123 — 135

To link to this Article: DOI: 10.1080/00319109408029517

URL: http://dx.doi.org/10.1080/00319109408029517

Phys. Chem. Liq., 1994, Vol. 27, pp. 123–135
Reprints available directly from the publisher
Photocopying permitted by license only

CHARGE ORDERING AND SIZE EFFECTS IN THE STRUCTURE OF A MODEL 2:1 IONIC COMPOUND

J. BORONAT

Departament de Física i Enginyeria Nuclear, Universitat Politècnica de Catalunya, Pau Gargallo 5, E-08028 Barcelona, Spain

M. SILBERT

School of Physics, University of East Anglia, Norwich NR4 7TJ, U.K.

(Received 12 May 1993)

A detailed study has been carried out of the effects arising as a result of the size difference and charge ordering in the structure of 2:1 ionic compounds. Calculations of both the Ashcroft–Langreth and Bhatia–Thornton have been performed within the Mean Spherical Approximation for a 2:1 compound of charged hard spheres.

KEY WORDS: 2:1 Ionic compounds, structure.

1 INTRODUCTION

The work by Abramo *et al.*[1] has served for many years as a very useful benchmark in the analysis and understanding of the structure of 1:1 ionic fluids. Their work has also shown that, in spite of its shortcomings, the Mean Spherical Approximation[2] (MSA) is a very useful tool for obtaining qualitative information on the competing effects between size difference and charge ordering in characterising the structure of these systems.

The interest has more recently widened with systematic experimental studies of 2:1 ionic fluids[3,4]. Here again the competing effects of size difference and charge ordering are assumed to be responsible for behaviour ranging from simple molten salts, to superionic liquids to good glass formers[2]. In some of these systems, under favourable conditions, intermediate range order (IRO) sets in[4]. Iyetomi and Vashishta[5] have recently studied the effects on the structure arising from the size difference between the ions in the two species of a 2:1 ionic compound and speculated on the conditions required for reproducing features in the partial structure factors which may be regarded as characteristic of IRO. Their calculations have used the MSA and hypernetted chain approximations[2] for charged hard spheres with values of the packing fraction and plasma coupling parameter which are regarded as typical of $GeSe_2$[6].

In this work we present a full MSA study of both ionic size difference and charge ordering effects on the structure of 2:1 ionic compounds, at constant packing fraction and temperature. We expect that the results of the calculations presented below will fulfill the same role for 2:1 ionic melts as those of Abramo *et al.*[1] for the 1:1 ionic liquids. We note, however, that it is not the purpose of this work to make direct contact with experimental results.

In the next section we summarize the results for the MSA and introduce both the Ashcroft–Langreth[7] (AL) and Bhatia–Thornton[7] (BT) partial structure factors. The following section is devoted to the presentation of our results. Finally, a summary of this work is presented.

2 MSA FOR CHARGED SPHERES

The potentials of interaction for charged hard spheres are given by

$$\phi_{ij}(r) = \begin{cases} \infty & \text{for} \quad r < (\sigma_i + \sigma_j)/2 \\ \dfrac{Z_i Z_j e^2}{4\pi\varepsilon_0 r} & \text{for} \quad r > (\sigma_i + \sigma_j)/2, \end{cases} \tag{1}$$

where the σ_i, Z_i are, respectively, the hard core diameter and charge of the spheres of species i. The latter satisfy the overall charge neutrality condition

$$x_1 Z_1 + x_2 Z_2 = 0, \tag{2}$$

where x_i is the concentration in number of the spheres of species i, such that $x_1 + x_2 = 1$.

The Mean Spherical Approximation (MSA) solves the Ornstein–Zernike equation

$$h_{ij}(r) = c_{ij}(r) + \rho \sum_l x_l \int d\mathbf{r}' \; c_{il}(r') h_{lj}(|\mathbf{r} - \mathbf{r}'|) \tag{3}$$

with the closure

$$h_{ij}(r) = -1 \qquad \text{for } r < (\sigma_i + \sigma_j)/2 \tag{4}$$

$$c_{ij}(r) = -\beta\phi_{ij}(r) \qquad \text{for } r > (\sigma_i + \sigma_j)/2. \tag{5}$$

In Equation (3) ρ is the total number density, $h_{ij}(r)$ denotes the total correlation function, and $c_{ij}(r)$ is the Ornstein–Zernike direct correlation function. In Equation (5) β is the inverse of the Boltzmann constant k_B times the temperature T. The MSA, for the potentials given by (1), has been solved analytically by Blum[8].

The species-species or AL partial structure factors $S_{ij}(k)$ may be defined in terms of the Fourier transforms of the $c_{ij}(r)$,

$$\tilde{c}_{ij}(k) = 4\pi\rho \int_0^\infty dr\, r^2 c_{ij}(r) \frac{\sin kr}{kr} \tag{6}$$

as

$$S_{ij}^{-1}(k) = \delta_{ij} - (x_i x_j)^{1/2} \tilde{c}_{ij}(k) \tag{7}$$

where δ_{ij} is the Kronecker delta.

The structural correlations may also be studied in terms of the charge fluctuations (the charge-charge partial structure factors $S_{ZZ}(k)$), density fluctuations (number-number partial structure factor $S_{NN}(k)$), and the cross density-charge fluctuations (the number-charge partial structure factor $S_{NZ}(k)$). In terms of the $S_{ij}(k)$ these, the BT partial structure factors, read[7]

$$S_{ZZ}(k) = \sum_i \sum_j (x_i x_j)^{1/2} Z_i Z_j S_{ij}(k), \tag{8}$$

$$S_{NN}(k) = \sum_i \sum_j (x_i x_j)^{1/2} S_{ij}(k), \tag{9}$$

and

$$S_{NZ}(k) = \sum_i \sum_j (x_i x_j)^{1/2} Z_j S_{ij}(k). \tag{10}$$

We present the results of calculations for both the AL and BT partial structure factors in the next section.

3 RESULTS

We consider 2:1 charged hard spheres, such that the packing fraction $\eta = 0.33$ and the temperature $T = 1000$ K. The former is defined by

$$\eta = \frac{1}{6} \pi\rho\sigma_2^3 (x_1\alpha^3 + x_2), \tag{11}$$

where $\alpha = \sigma_1/\sigma_2$. In all cases σ_2, the unit of length in our calculations, is the diameter of the larger sphere. We have carried out calculations for $\alpha = 1.0$, 0.8, 0.6, 0.4 and 0.2. We have studied both the cases when the smaller sphere carries the smaller charge, in which case $x_1 = \frac{2}{3}$, and the converse namely when the smaller sphere carries the larger charge, in which case $x_1 = \frac{1}{3}$. Thus we have studied the cases $|Z_1| = 0.2$, 0.4, 0.6, 0.8, 1.0, 1.2, 1.6 and 2.0.

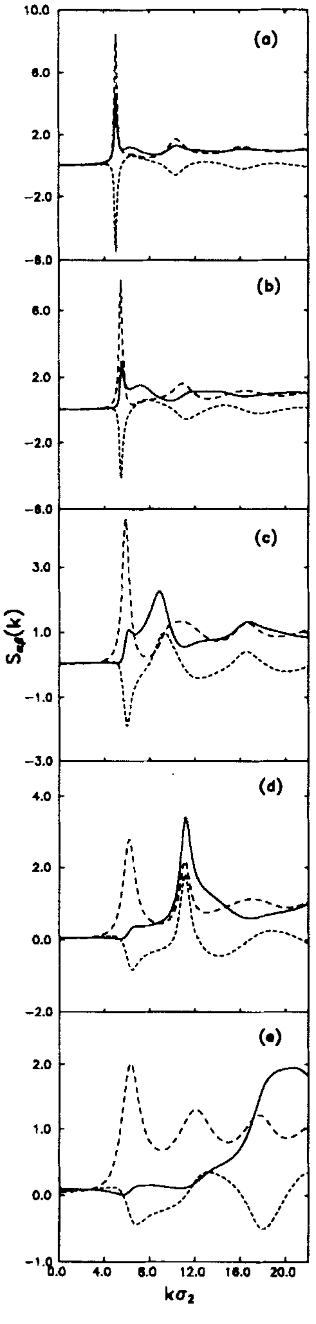

Figure 1 Ashcroft-Langreth partial structure factors. Effects due to size difference for $|Z_1| = 1.0$. Solid line, $S_{11}(k)$; long-dashed line, $S_{22}(k)$; short-dashed line, $S_{12}(k)$. (a) $\alpha = 1.0$; (b) $\alpha = 0.8$; (c) $\alpha = 0.6$; (d) $\alpha = 0.4$; (e) $\alpha = 0.2$.

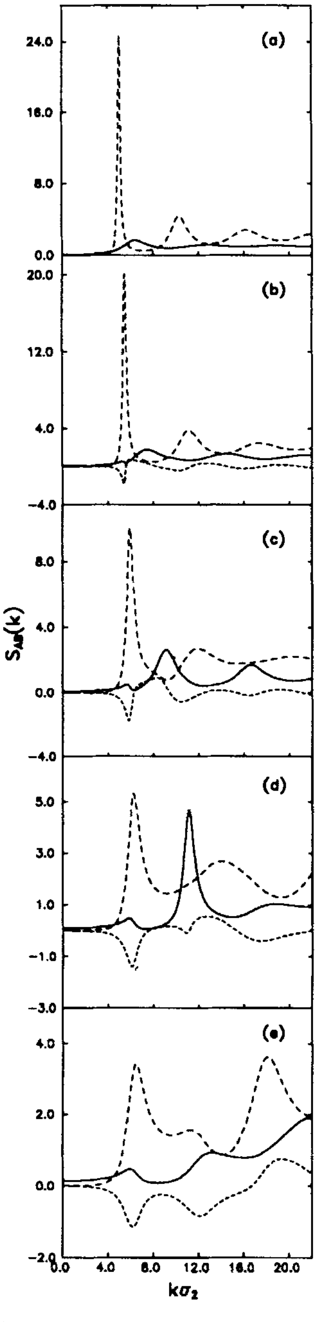

Figure 2 Bhatia-Thornton partial structure factors. Effects due to size difference for $|Z_1| = 1.0$. Solid line, $S_{NN}(k)$; long-dashed line, $S_{ZZ}(k)$; short-dashed line, $S_{NZ}(k)$. (a) $\alpha = 1.0$; (b) $\alpha = 0.8$; (c) $\alpha = 0.6$; (d) $\alpha = 0.4$; (e) $\alpha = 0.2$.

The discussion below is limited to a selected number of representative examples. A full set of figures is available on request.

First we present the result of the effects arising from the size difference between the spheres when the ions are fully charged. Figures 1 and 2 show, respectively, the AL and BT partial structure factors for $|Z_1| = 1.0$, $|Z_2| = 2.0$.

For $\alpha = 1.0$ we find complete Coulomb ordering, as shown in Figure 1(a), with the positions of the first peaks maxima of $S_{11}(k)$ and $S_{22}(k)$ and first minimum of $S_{12}(k)$ all at $k\sigma_2 \simeq 5.0$. We note that the magnitude of the $S_{22}(k)$ peak height, the partial of the species with the lower concentration, is the largest. $S_{11}(k)$ has a somewhat extended second peak. As α is reduced the first peak heights of $S_{11}(k)$ and $S_{22}(k)$ and first minimum of $S_{12}(k)$ are lower and broader, with a shift in their positions towards larger $k\sigma_2$, more for $S_{11}(k)$ and $S_{12}(k)$ than for $S_{22}(k)$. The second peak of $S_{11}(k)$ becomes more pronounced and, in going from $\alpha = 0.8$ to $\alpha = 0.6$, there is a qualitative change as the second peak of $S_{11}(k)$ becomes higher than the first. Moreover, for $\alpha = 0.4$ there appear to be two competing effects, one at $k\sigma_2 \gtrsim 6.0$ the other at $k\sigma_2 \gtrsim 11.0$, which on inspection of Figure 2(d) are clearly shown as pertaining to charge fluctuations, $S_{ZZ}(k)$, and density fluctuations, $S_{NN}(k)$. These are known in the field of liquid alloys as chemical short range order (CSRO) and topological short range order (TSRO)[9]. Turning to the BT partials we find that for $\alpha = 1.0$ $S_{ZZ}(k)$, namely CSRO, is the dominant feature with a sharp high first peak, whereas $S_{NN}(k)$ has a comparatively lower and broader first peak at a larger value of $k\sigma_2$. As α is reduced $S_{NZ}(k)$ starts contributing and $S_{NN}(k)$ develops a prepeak on the lower k side of its first peak which becomes more pronounced for smaller values of α. As indicated for the AL partials there is also a qualitative change in going from $\alpha = 0.8$ to $\alpha = 0.6$. However going from $\alpha = 0.4$ to $\alpha = 0.2$ the two strongly competing CSRO and TSRO effects present at $\alpha = 0.4$ are considerably weaker.

We now turn to the case when the smaller ion carries the large charge and the ions are still fully charged. The results shown in Figures 3 and 4 are not symmetrical to those discussed above. For $\alpha = 0.8$, $S_{11}(k)$ and $S_{12}(k)$ are almost in antiphase, with the position of the first maximum of $S_{11}(k)$ and first minimum of $S_{12}(k)$ at a slightly larger value than the first peak of $S_{22}(k)$. The latter is broader and exhibits a shoulder on its high k side.

We also find a qualitative change in going from $\alpha = 0.8$ to $\alpha = 0.6$ with a pronounced shift in the position of the first peak of $S_{11}(k)$ towards a higher value of k, $k\sigma_2 \simeq 8.0$, and a shoulder now on its lower k side. The position of the first minimum of $S_{12}(k)$ has also shifted towards about the same position as the shoulder in $S_{11}(k)$, while the now broader first peak of $S_{22}(k)$ has its position only slightly shifted towards $k\sigma_2 \simeq 6.0$. For $\alpha = 0.4$ we find again two competing effects, one at $k\sigma_2 \gtrsim 6.0$ dominated by the first peak of $S_{22}(k)$, the other at $k\sigma_2 \simeq 11.0$ where the three partials contribute, although the first peak of $S_{11}(k)$ is its dominant feature. On inspection of the BT partials we note that, as shown in Figure 4(c), now the three partials contribute to the two competing effects, only that at lower k it is the first minimum of the cross-correlation, while at higher k its first maximum which contribute to these two competing effects. We also note, as shown in Figure 4(a, b) that in changing from $\alpha = 0.8$ to $\alpha = 0.6$ the first peak of $S_{ZZ}(k)$ splits into two,

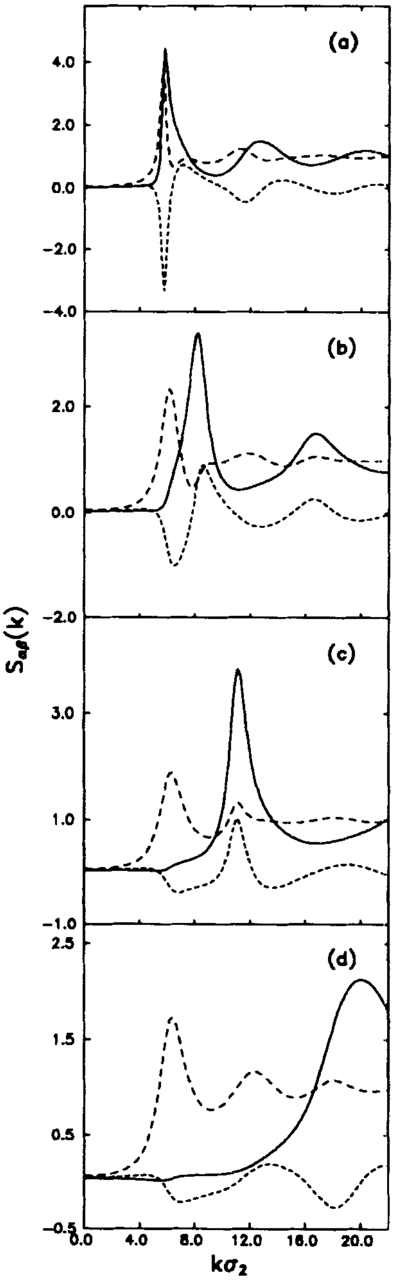

Figure 3 Same caption as in Figure 1 but for $|Z_1| = 2.0$. (a) $\alpha = 0.8$; (b) $\alpha = 0.6$; (c) $\alpha = 0.4$; (d) $\alpha = 0.2$.

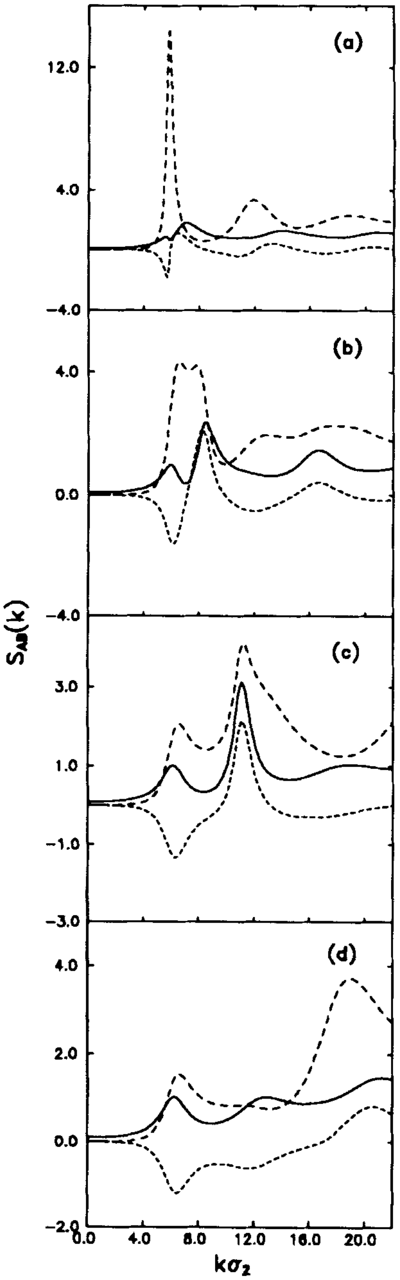

Figure 4 Same caption as in Figure 2 but for $|Z_1| = 2.0$. (a) $\alpha = 0.8$; (b) $\alpha = 0.6$; (c) $\alpha = 0.4$; (d) $\alpha = 0.2$.

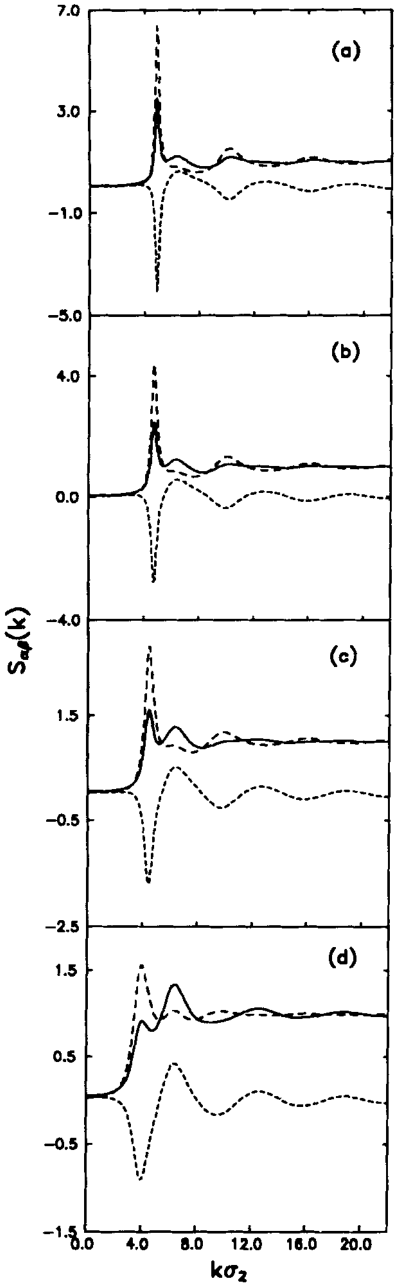

Figure 5 Ashcroft-Langreth partial structure factors. Effects due to charge ordering for $\alpha = 1.0$. Solid line, $S_{11}(k)$; long-dashed line, $S_{22}(k)$; short-dashed line, $S_{12}(k)$. (a) $|Z_1| = 0.8$; (b) $|Z_1| = 0.6$; (c) $|Z_1| = 0.4$; (d) $|Z_1| = 0.2$.

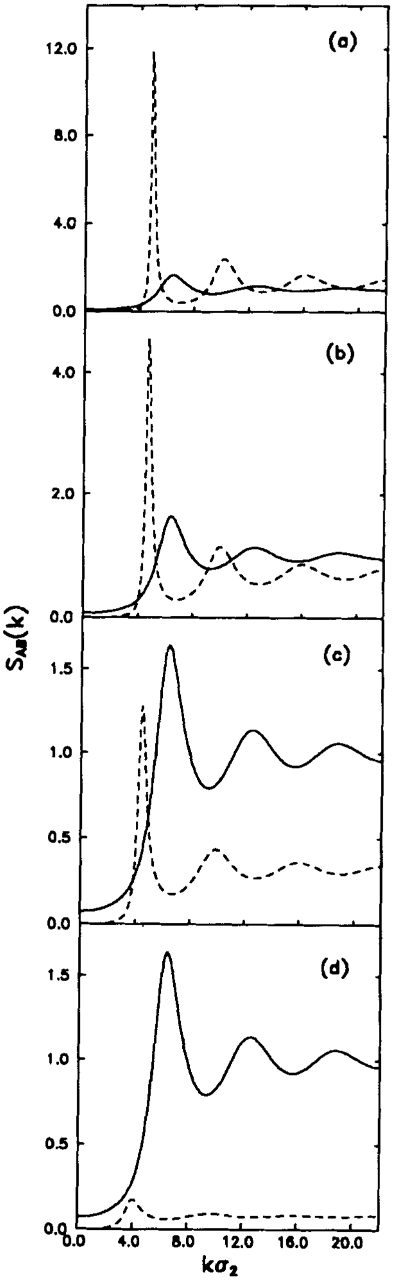

Figure 6 Bhatia-Thornton partial structure factors. Effects due to charge ordering for $\alpha = 1.0$. Solid line, $S_{NN}(k)$; long-dashed line, $S_{ZZ}(k)$; short-dashed line, $S_{NZ}(k)$. (a) $|Z_1| = 0.8$; (b) $|Z_1| = 0.6$; (c) $|Z_1| = 0.4$; (d) $|Z_1| = 0.2$.

and the two peaks become better defined as the size difference between the spheres increases.

We now study the effects arising from the incomplete ionization of the ions. The results, for $\alpha = 1.0$, are shown in Figures 5 and 6. When the size of the ions is the same charge cancellation, as indicated by the positions in phase of the first peaks of $S_{11}(k)$ and $S_{22}(k)$ and the first minimum of $S_{12}(k)$, is preserved up to values of $|Z_1| = 0.4$ as shown in Figure 5(a,b,c). These peaks broaden as the charges are reduced but their positions are unchanged. An important change appears when $|Z_1| = 0.2$, as shown in Figure 5(d). The positions of the first peaks are still in phase but are now shifted to a smaller value of k, $k\sigma_2 \simeq 4.0$, and a competing effect appears at about $k\sigma_2 = 6.4$ where both the second peaks of $S_{11}(k)$ and $S_{22}(k)$ are in phase with the first peak of $S_{12}(k)$. The case $\alpha = 1$ is also interesting in that $S_{NZ}(k) = 0$ for all k in the MSA. Hence only the competing CSRO and TSRO effects are present. We find that for $|Z_1| = 0.8$ and 0.6, $S_{ZZ}(k)$ is the dominant feature as shown in Figure 6(a,b), although the first peak is lower and broader as the charges are reduced. As expected the reverse trend is found for $S_{NN}(k)$ with the first peak becoming more pronounced as the charges are reduced, so that for $|Z_1| = 0.4$ the first peak maximum of $S_{NN}(k)$ is higher than $S_{ZZ}(k)$, as seen in Figure 6(c), and for $|Z_1| = 0.2$ $S_{NN}(k)$ becomes the dominant structural correlation.

The case when species 1 carries the larger charge for $\alpha = 1$ is symmetrical to that discussed above, except that we have to exchange the role of $S_{11}(k)$ and $S_{22}(k)$, and therefore we omit the corresponding figures and discussion.

We now return to study the effects due to the size difference between the ions for two particular cases of incomplete ionization, namely $|Z_1| = 0.6$, shown in Figures 7 and 8, and $|Z_1| = 1.2$, shown in Figures 9 and 10.

When $|Z_1| = 0.6$ charge ordering is quickly eroded with increasing size difference. The first effect is always present at lower values of k, but already for $\alpha = 0.6$ the second peak maximum of $S_{11}(k)$ is higher than the first peak, as shown in Figure 6(b). The two competing effects are clearly shown in Figure 7(b) with the first peaks of $S_{ZZ}(k)$ and $S_{NN}(k)$ clearly dominant, the first at $k\sigma_2 \simeq 5.6$, the second at $k\sigma_2 \simeq 8.8$, although $S_{NN}(k)$ exhibits a prepeak on the lower k side, which becomes more pronounced, and whose position shifts towards smaller values of k, as the size difference increases. The positions of the main peaks of $S_{ZZ}(k)$ and $S_{NN}(k)$ shift towards larger values of k. For $\alpha = 0.2$ we find the three partials contributing to both effects, as shown in Figure 8(c), a reflection of the large fluctuations present.

When $|Z_1| = 1.2$ the position of the first peak of $S_{11}(k)$, which for $\alpha = 0.8$ almost coincides with that of $S_{22}(k)$ (Figure 9(a)), shifts towards larger values of k with increasing size difference. The shift of the position of the first peak of $S_{22}(k)$ towards larger k is much smaller, from $k\sigma_2 \simeq 5.4$ to 6.4 as α changes from 0.8 to 0.2, so that the two peaks are clearly identificable for $\alpha = 0.4$ (shown in Figure 13(b)). $S_{11}(k)$ exhibits a shoulder on the high k side of the first peak for $\alpha = 0.8$, turning into a shoulder on the low k side for $\alpha = 0.6$, and finally becoming a broad prepeak for $\alpha = 0.2$. Turning to the BT partials we note that only for $\alpha = 0.8$ is $S_{ZZ}(k)$ the dominant feature. As the size difference between the ions increases there are two competing effects in which all partials contribute, which is more marked for $\alpha = 0.4$ (shown in Figure 14(b)).

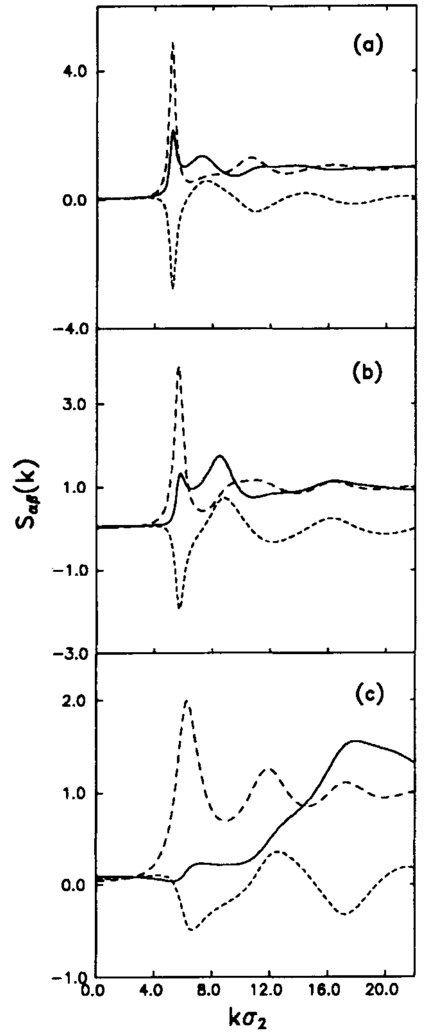

Figure 7 Same caption as in Figure 1 but for $|Z_1| = 0.6$. (a) $\alpha = 0.8$; (b) $\alpha = 0.6$; (c) $\alpha = 0.2$.

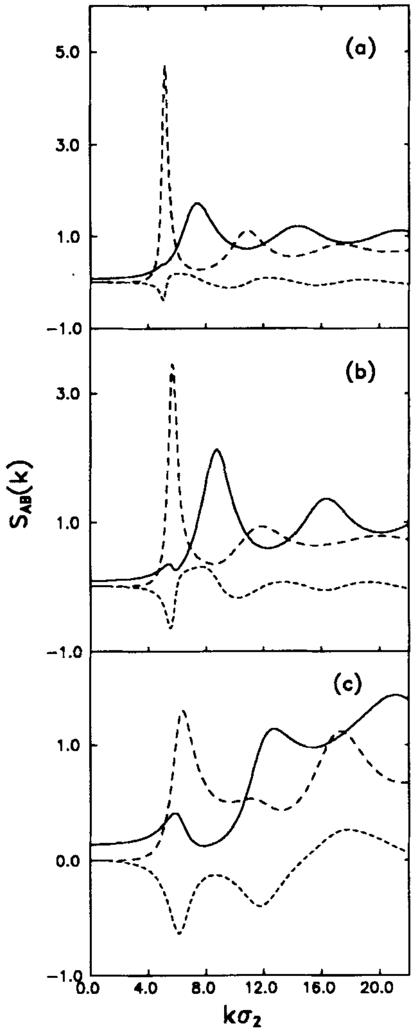

Figure 8 Same caption as in Figure 2 but for $|Z_1| = 0.6$. (a) $\alpha = 0.8$; (b) $\alpha = 0.6$; (c) $\alpha = 0.2$.

Finally we turn to the effect arising from charge ordering at a fixed size difference $\alpha = 0.4$. We consider both the cases when the smaller ion carries the smaller charge, Figures 11 and 12, and when it carries the larger charge, Figures 13 and 14.

Figure 11 shows the AL partial structure features as the charges are reduced from $|Z_1| = 0.8$ to 0.2. For $|Z_1| = 0.8$ we observe two main features, as shown in Figure 11(c), one at $k\sigma_2 \simeq 5.3$ the other at $k\sigma_2 \simeq 10.7$. The first peak of $S_{22}(k)$, a prepeak of $S_{11}(k)$ and the first minimum of $S_{12}(k)$ contribute to the first; the first peaks of $S_{11}(k)$ and $S_{12}(k)$ and the second peak of $S_{22}(k)$ contribute to the second. Similar correlations are found for $|Z_1| = 0.6$ and 0.4, with the prepeak of $S_{11}(k)$ more pronounced and a weaker second feature. For $|Z_1| = 0.2$ the second feature has

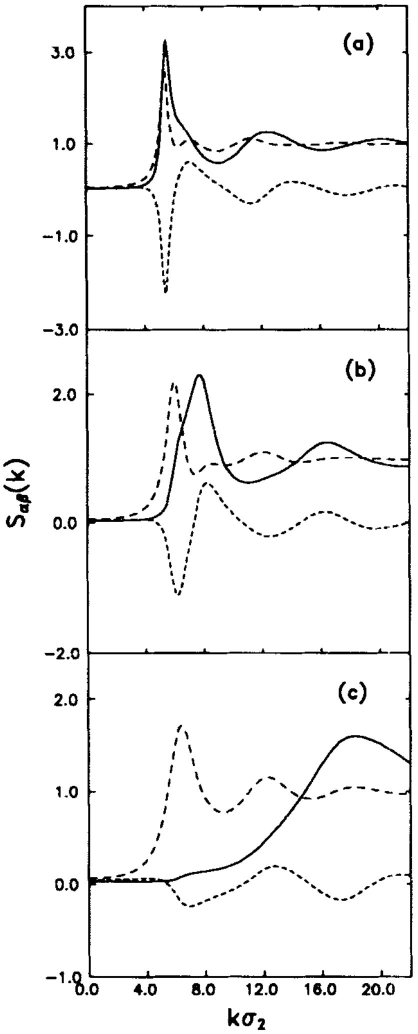

Figure 9 Same caption as in Figure 1 but for $|Z_1| = 1.2$. (a) $\alpha = 0.8$; (b) $\alpha = 0.6$; (c) $\alpha = 0.2$.

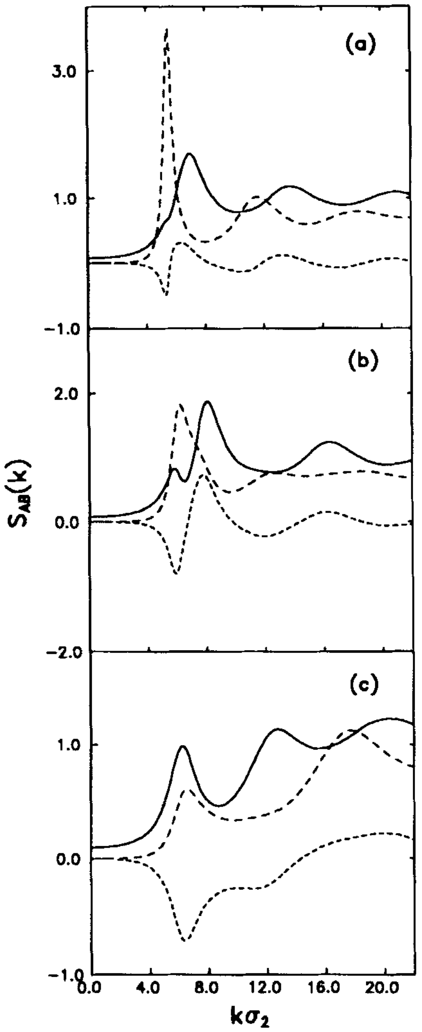

Figure 10 Same caption as in Figure 2 but for $|Z_1| = 1.2$. (a) $\alpha = 0.8$; (b) $\alpha = 0.6$; (c) $\alpha = 0.2$.

almost gone. The BT partials, shown in Figure 12, identify these two features as the competition between charge and density fluctuations, the first becoming weaker at the expense of the second as the charges are decreased. For $|Z_1| = 0.2$ $S_{NN}(k)$ is the main correlation.

This picture is significantly altered at the level of the BT partials, when the smaller ion carries the larger charge, as shown in Figure 14. Here there are also two main features, one at $k\sigma_2 \gtrsim 6.0$ the other at $k\sigma_2 \simeq 11.0$, but all three partials contribute to both. Both features become weaker as the charge is decreased. For $|Z_1| = 0.4$ $S_{NN}(k)$ is again the main correlation exhibiting a very broad first peak which incorporates both the prepeak and first peak present at larger charges.

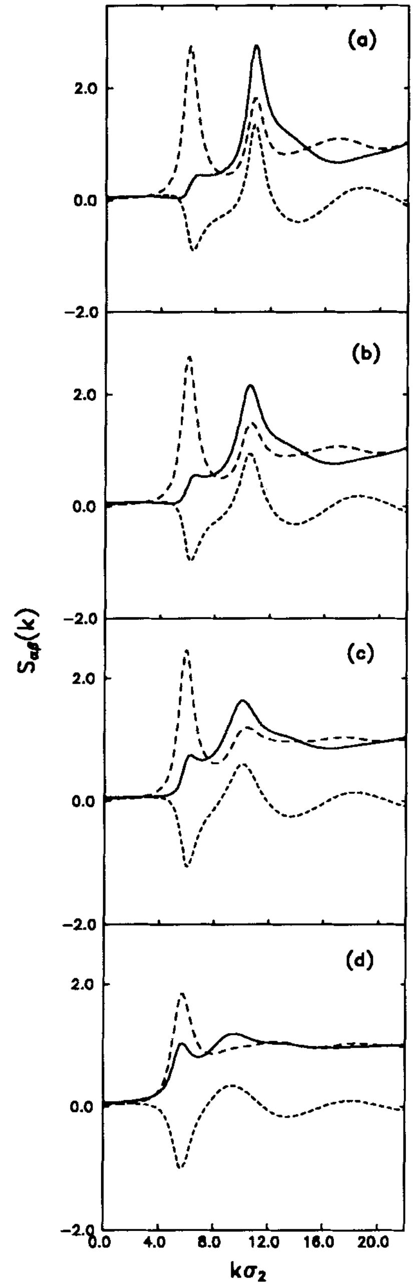

Figure 11 Same caption as in Figure 5 but for $\alpha = 0.4$. (a) $|Z_1| = 0.8$; (b) $|Z_1| = 0.6$; (c) $|Z_1| = 0.4$, $|Z_2| = 0.8$; (d) $|Z_1| = 0.2$.

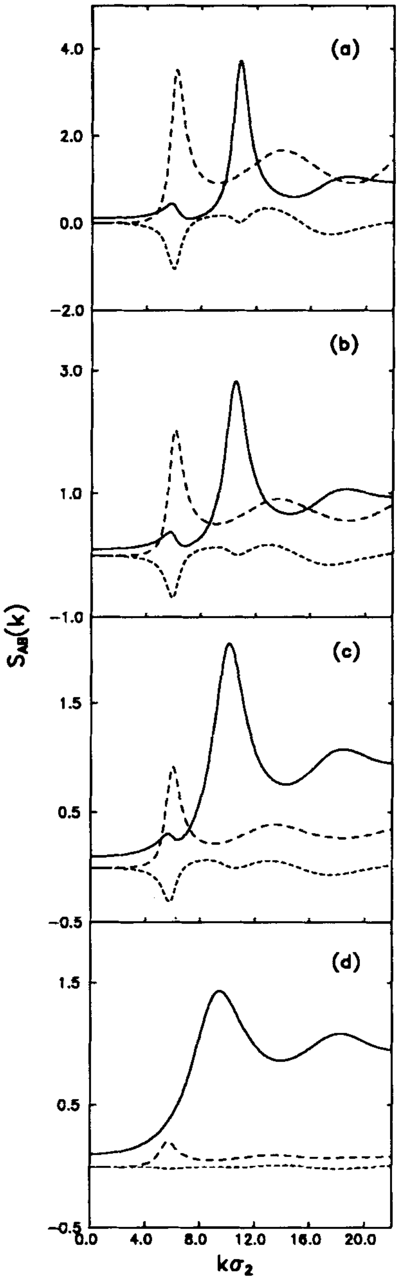

Figure 12 Same caption as in Figure 6 but for $\alpha = 0.4$. (a) $|Z_1| = 0.8$; (b) $|Z_1| = 0.6$; (c) $|Z_1| = 0.4$, $|Z_2| = 0.8$; (d) $|Z_1| = 0.2$.

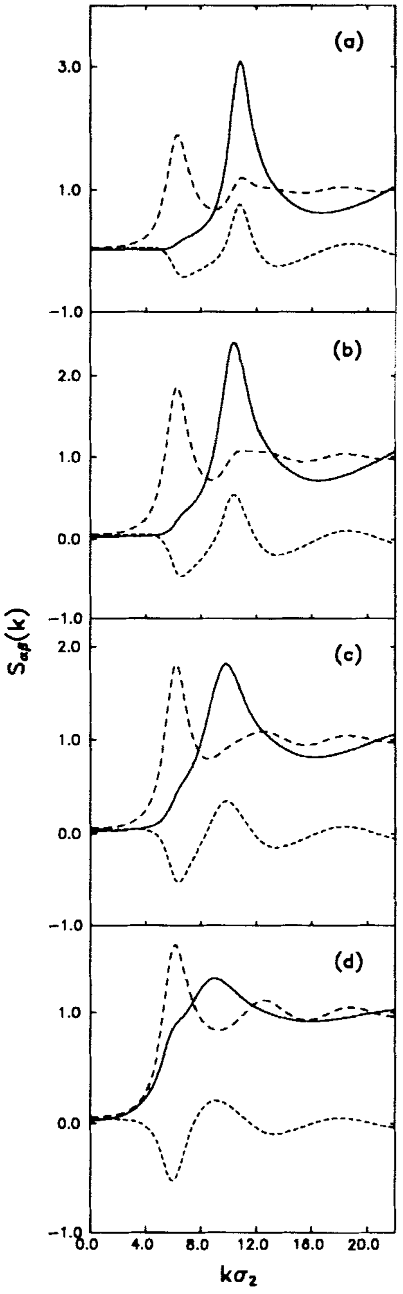

Figure 13 Same caption as in Figure 5 but for $\alpha = 0.4$. (a) $|Z_1| = 1.6$; (b) $|Z_1| = 1.2$; (c) $|Z_1| = 0.8$; (d) $|Z_1| = 0.4$, $|Z_2| = 0.2$.

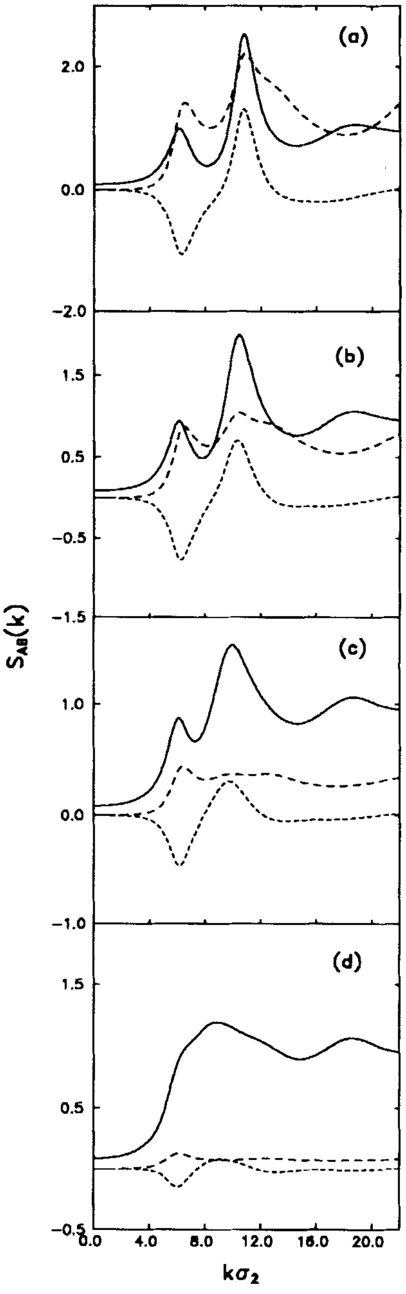

Figure 14 Same caption as in Figure 6 but for $\alpha = 0.4$. (a) $|Z_1| = 1.6$; (b) $|Z_1| = 1.2$; (c) $|Z_1| = 0.8$; (d) $|Z_1| = 0.4$, $|Z_2| = 0.2$.

4 CONCLUSIONS

March and Tosi[2] noted that in the case of 2:1 ionic compounds it becomes necessary to examine the behaviour of the two (coupled) ionic components. In this work we have shown that this behaviour, as a function of both the size difference and the magnitude of the charges, is very rich even in a simple model of charged hard spheres. The results of our calculations for the Ashcroft–Langreth and Bhatia–Thornton partial structure factors clearly exhibit the competition between size and charge effects which have been identified by many authors[5,9] as the main ingredients for the onset of Intermediate Range Order in these liquids. We have deliberately refrained from providing an interpretation of our results and have only commented on the distinctive features of the representative set of results presented in this work. These are only intended as a "guide to the eye" for both experimentalists and theorists in the assessment and interpretation of their own results.

Acknowledgements

It is a pleasure to thank Professor Antoni Giró and Dr. Phil Salmon for useful discussions. One of us (M.S.) thanks the hospitality of the Departament de Física i Enginyeria Nuclear of the Universitat Politècnica de Catalunya, during a research visit when this work was completed. This work has been supported in part by DGICYT (Spain) Grants No. PB89-0332 and No. PB90-06131.

References

1. M. C. Abramo, C. Caccamo, G. Pizzimenti, M. Parrinello and M. P. Tosi, *J. Phys. C* **9**, L593 (1976); *J. Chem. Phys.* **68**, 2889 (1978); M. C. Abramo, C. Caccamo, G. Pizzimenti, *Phys. Chem. Liq.* **6**, 167 (1977).
2. See, c.f., N. H. March and M. P. Tosi, *Coulomb Liquids* (Academic Press, London 1984).
3. R. L. McGreevy, *Solid State Phys.* **40**, 287 (1987).
4. P. S. Salmon, *Proc. R. Soc. London A* **437**, 591 (1992).
5. H. Iyetomi and P. Vashishta, *Phys. Rev. B* **47**, 3063 (1993).
6. H. Iyetomi, P. Vashishta and R. L. Kalia *Phys. Rev. B.* **43**, 1726 (1991).
7. See, c.f., J. P. Hansen in *Amorphous Solids and the Liquid State*, Eds. N. H. March, R. A. Street and M. P. Tosi (Plenum Press, 1985), pp 229–280.
8. L. Blum, *Mol. Phys.* **30**, 1529 (1975). See also K. Hiroike, *ibid* **33**, 119 (1977).
9. We adopt here the definition given, e.g., in M. L. Saboungi, W. Geertsma and D. L. Price, *Annu. Rev. Phys. Chem.* **41**, 207 (1990).